Effects of sizing on battery life and generation cost in PV–wind battery hybrid systems

Mayur P. Bonkile, Venkatasailanathan Ramadesigan *

Department of Energy Science and Engineering, Indian Institute of Technology Bombay, India

ARTICLE INFO

ABSTRACT

Battery energy storage system (BESS) is a crucial part of standalone renewable hybrid power systems. Dynamic battery degradation analysis and life prediction are essential for better techno-economic estimation of standalone PV–wind battery hybrid power systems. With this viewpoint, this paper aims to study battery degradation using a physics-based pseudo-two-dimensional (P2D) thermal battery model integrated with renewable PV–wind hybrid power systems and investigates the impact of BESS size variation on its degradation and its effect on the energy generation costs A power management and control strategy is developed to ensure continuous power flow with two regulation modes; (a) maximum power point tracking and (b) controlled power generation. Yearly real-world load data, operating, and ambient conditions are used to study five different percentage mixes of PV and wind power generation scenarios. For example, a mix of 70% PV-30% wind, 350 kWh BESS is needed (base case) based on the demand. The yearly degradation rate for this case is calculated to be 3.80%. The degradation rates vary from 3.80 to 2.33% per year for every 10% increment in the BESS size from the base case. Performing a techno-economic analysis reveals that the least energy generation cost is achieved when increasing the BESS size by 20%. This increases BESS life from 5.3 years to 7.3 years and reduces the generation cost from 35.19 ₹ kWh^{-1} (0.482 \$ kWh^{-1}) to 34.34 ₹ kWh^{-1} (0.470 \$ kWh^{-1}). These results provide essential insights to analyse the impact of BESS sizing on degradation and energy generation cost in a standalone PV–wind battery hybrid power system framework. The oversized BESS provides extended life and reduces the energy generation cost for a standalone PV–wind–battery hybrid power system.

1. Introduction

The rising population and economic development escalated the global energy demand by 120 million tonnes of oil equivalent in 2019, as per the global energy review 2019 report (IEA, 2020). A major part (nearly 86%) of this energy was generated from fossil fuels, e.g., coal, natural gas, and oil (Bakay and Ümit Ağbulut, 2021). These energy sources are limited, and the uncontrolled consumption to satisfy the growing energy demand results in greenhouse gas emissions. Sustainable energy generation using renewable resources like solar and wind provide an alternative clean option (Altun and Kilic, 2020). Feasible and sustainable combinations of different renewable power systems can provide power to the unelectrified villages based on site conditions and load demand (Mazzeo et al., 2021). The combination of solar-PV panels and wind turbines can harness maximum renewable energy and improve the power systems' reliability (Sreeraj et al., 2010). A standalone solar-PV–wind hybrid power system can be a better alternative to generate and supply power at remote locations as grid extension may

not always be a financially attractive option considering factors like distance, end-users demand, and emissions (Ortega-Arriaga et al., 2021). The energy storage system is becoming a crucial part of standalone PV–wind hybrid power systems due to intermittent nature of power generation and for aiding in various operations like frequency regulation, voltage support, and peak shaving (Koohi-Fayegh and Rosen, 2020). Balducci et al. (2018) presented a detailed literature review to study various benefits provided by energy storage systems. Cebulla et al. (2018) studied the US, European and German electricity markets to calculate energy storage requirement based on renewable energy generation share. They found that the energy storage systems capacity increases linearly with renewable energy share after examining 17 storage expansion studies. India has committed 175 GW of renewable energy generation by 2022 and could be expanded to 400–500 GW by 2030, which needs energy storage systems for a reliable, stable and low carbon grid. India's total energy storage demand for renewable

---

integration and electric transportation is estimated to be more than 2416 GWh by 2032 (NITI Aayog, 2021).

The standalone PV–wind hybrid power systems are usually installed with battery energy storage to improve the power system's reliability, and efficiency (Fragaki et al., 2019; Hannan et al., 2020). Secondary lithium-ion batteries are an excellent choice for battery energy storage in standalone PV–wind hybrid power systems (Rallo et al., 2020; Koohi-Fayegh and Rosen, 2020). Though a considerable fall in renewable technologies' price is observed in the past decade, the high cost of lithium-ion battery energy storage system (BESS) has slowed down their wider adoption (Cole and Frazier, 2019). The BESS is generally designed after carefully analysing renewable power generation and load demand for a particular location. The design optimisation of such hybrid power systems to reduce energy generation costs is a rapidly growing research area. Arabi-Nowdeh et al. (2021) compared the performance of PV–wind–battery and wind–battery hybrid power systems considering the cost of emissions, penalty of load losses and a few reliability indices. Their results showed the PV–wind–battery hybrid power system to be the best. Roy et al. (2007, 2009) proposed a design-space methodology for size optimisation of a standalone renewable hybrid power system. From the design-space approach, the minimum cost of energy was calculated for a particular location. Ghorbani et al. (2018) carried out the cost-reliability optimisation of PV–wind battery hybrid power systems using a hybrid genetic algorithm with particle swarm optimisation method. The optimal BESS capacity was reduced to 190 kWh from 350 kWh, thus reducing the levelized cost of energy. Kumar and Saini (2020) investigated the financial feasibility using the salp swarm algorithm, optimising the energy storage capacity from 882 kWh to 772 kWh. Murugaperumal and Ajay D. Vimal Raj (2019) implemented artificial neural network feedback propagation and Levenberg–Marguardt technique for load growth forecasting to reduce the number of batteries from 1200 to 800, decreasing the cost of energy from 11.33 ₹ kWh^{-1} to 10.18 ₹ kWh^{-1}. Li et al. (2020) calculated the cost of energy as 2.31 \$ kWh^{-1} using HOMER for a renewable power system with lithium-ion battery storage. Al-Sharafi et al. (2017) optimised and simulated different renewable hybrid power systems in HOMER and calculated the levelized cost of energy of 0.779 \$ kWh^{-1} for the PV–battery system, 0.848 \$ kWh^{-1} for the wind–battery system, and 0.702 \$ kWh^{-1} for the PV–wind battery system. As discussed above, the ratings of renewable sources and BESS were determined and optimised by various researchers while designing renewable hybrid power systems. It can be concluded that the optimum BESS size was always found to be lower than the base case. The battery energy storage capacity reduces during the charging–discharging process due to continuous degradation. Generally, the battery degradation and actual life are neglected while optimising and calculating the energy generation cost of PV–wind battery hybrid power systems. The deployment of BESS is always associated with high investment, and therefore system optimisation neglecting dynamic battery degradation will not be sufficient to improve financial feasibility. Thus it becomes necessary to analyse the impact of battery degradation on the energy generation cost of renewable hybrid power systems.

The interdependence among BESS size, degradation, and energy generation cost is considered in a standalone PV–wind battery hybrid power system in this work. This can be achieved through physics-based battery models as they consider the complex physio-chemical processes happening inside the battery, provide better insight into the battery behaviour, and estimate the accurate battery performance (Onori and Lee, 2019; Rahimian et al., 2011). The physics-based P2D thermal battery model is used that includes mass, energy, and charge conservation and reaction kinetics in the homogeneous solid and electrolyte phases, along with chemical degradation (Doyle et al., 1996; Ramadesigan et al., 2012). The harsh ambient and operating conditions can accelerate battery degradation, resulting from various chemical and physical processes co-occurring (Li et al., 2018). As a result, the battery loses its energy storage capacity with reduced life (Liu et al., 2019). The

battery degradation due to chemical and mechanical phenomena are impossible to observe during battery operation. However, its effect on capacity fade can be measured. The cell's internal resistance increases due to the degradation, and it is reflected in the voltage drop in response to the load profile (Harris et al., 2017). The battery capacity depends on the quantity of lithium-ions moving between the electrodes and their ability to host the ions. The loss of these moving lithium-ions, unavailability of the electrodes to hold them or both are attributed to irreversible capacity fade. The capacity fade may happen due to various reasons like solid electrolyte interface (SEI) layer formation, particle cracking, lithium plating, contact losses from corrosion, and structural disordering. Different degradation mechanisms affecting electrodes, electrolyte, separator and current collectors are interconnected and, therefore is very difficult to model all of them simultaneously (Birkl et al., 2017). The SEI layer formation, growth, decomposition and regeneration is one of the dominant battery degradation mechanisms widely studied in the literature (Peled, 1979; Peled et al., 1997) and is considered in this work. The battery state of charge (SoC), ambient and operating temperature, and load demand are the main external factors affecting battery degradation (Edge et al., 2021). Fayaz et al. (2021) have provided a state of the art review of various methods to control and maintain the thermal performance of lithium-ion batteries. The in-depth critical review highlighted optimisation techniques of thermal and structural design parameters under different battery thermal management systems. The impact of temperature on battery degradation and the thermal management and power control strategy for a standalone PV-BESS hybrid power system is analysed in our previous work (Bonkile and Ramadesigan, 2020). The rate of parasitic side reactions is related to the electrode potential, and degradation is more pronounced at higher battery SoC (Edge et al., 2021; Safari et al., 2009). Hence, SEI layer growth is more at higher battery SoC resulting in rapid degradation (Schimpe et al., 2018). One way to reduce the degradation is to reduce the operational time of the battery in the high SoC range. This can be achieved by oversizing the BESS, thereby preventing degradation to some extent. This simple but effective BESS sizing approach is implemented in this work, which helps to improve the battery life. The extra price of an oversized BESS adds to the initial investment cost; however, the improved battery life may lower the annualised life cycle cost. There would be a limit to adding additional BESS capacity to decrease degradation since, beyond a point, this might not be a cost-effective alternative. The trade-off between BESS sizing and the annualised life cycle cost is analysed in this work.

A majority of the research community is busy improving the lithium-ion battery's energy and power density by developing suitable battery chemistry and coming up with new materials. However, this work focuses on existing lithium-ion battery technologies to improve their performance, reliability, and economic feasibility by implementing robust control strategies. The present work mainly focuses on system-level performance and techno–economic analysis of PV–wind battery hybrid power systems. This work uses a physics-based P2D thermal lithium-ion battery model including SEI layer-based battery degradation to study its impact on the cost of energy generation in PV–wind battery hybrid power systems. Earlier work on renewable hybrid power systems reported in the literature either considered the dump load system and operation of renewable sources only at maximum power point (MPP) (Ghorbani et al., 2018) or enough explanation is not provided about power control strategy (Al-Sharafi et al., 2017). A power management and control strategy is designed for smooth and uninterrupted power flow in a PV–wind battery hybrid power system framework. The proposed power control algorithm can track solar-PV and wind turbine's maximum power point to generate maximum power or operate at a suitable condition to guarantee 0% dumping power. Five different scenarios of percentage mix of PV and wind turbine (WT) power generation (100% WT, 70% WT and 30% PV, 50% WT and 50% PV, 30% WT and 70% WT, 100% PV) are considered to investigate the proposed approach. Detailed techno–economic analysis
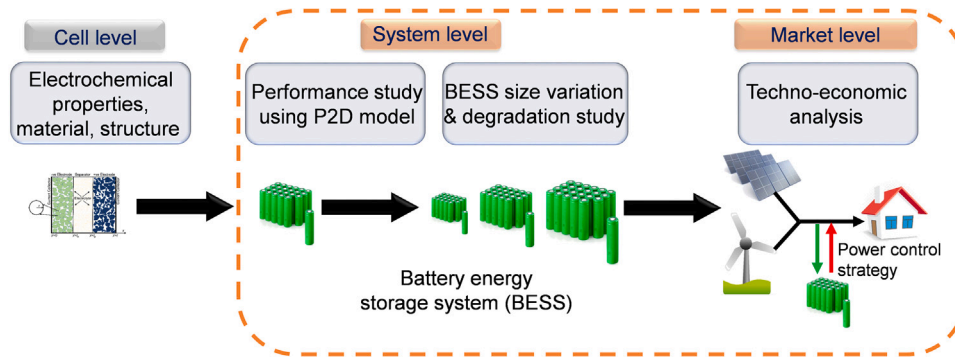
Fig. 1. Research methodology of this work.

and system simulations are performed to investigate the effect of BESS size variation on the battery degradation and energy generation cost. The annualised life cycle cost (ALCC) is calculated using the actual BESS life from simulation results instead of a constant life given by the manufacturer. The end of life condition for the battery is assumed to be a 20% degradation from its initial capacity (Schmalstieg et al., 2014). These simulation results can be used to decide the BESS size and reduce the cost of energy generation. The main contributions of the proposed work are highlighted in Fig. 1 and may be summarised as follows:

- An efficient and effective power management and control strategy is implemented to track and operate the hybrid power systems (both PV and wind) at maximum power point or deviate from it to guarantee zero dumped energy and avoid dumping load system
- Different mixes of PV–wind contribution in a hybrid power system framework with integrated BESS simulated for a year using real-world data for a small town in India
- A physics-based P2D thermal battery model to calculate SEI layer-based battery degradation in PV–wind battery hybrid power systems to perform a comprehensive analysis of BESS size variation and degradation on the energy generation cost of PV–wind battery hybrid power systems and BESS life
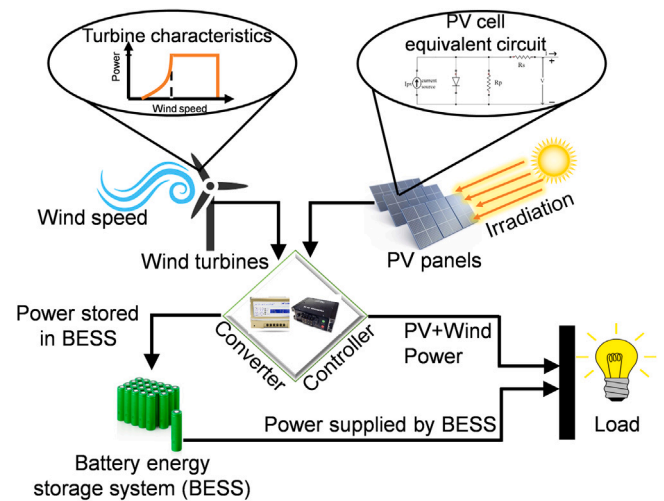
2. Framework overview and methodology

A standalone PV–wind battery hybrid power system comprises of solar-PV panels and wind turbines as power generation sources connected to a lithium-ion BESS. A schematic representation of the developed PV–wind battery hybrid power system framework is shown in Fig. 2. A brief overview of the system equations are given in Table 1. The power generated by the PV panel is calculated as described by Lee et al. (2017), and the wind turbine power is calculated using the equations provided by Deshmukh and Deshmukh (2008). The physics-based P2D thermal battery model used in this framework is described in detail by Torchio et al. (2016).

2.1. System framework

Kyocera KC200GT solar-PV panels (Kyocera, 2015) and Aeolos-V wind turbines (Aeolos, 2018) are considered for simulation with a rated output peak power of 200 W and 5 kW, respectively. The nominal short-circuit current and voltage of the solar cell is 8.21 A and 32.9 V. The swept area (A_{WT}) of the three-blade wind turbine is 15.9 m^2, cut-in wind speed is (V_{ci}=1.5 ms^{-1}), rated wind speed is (V_w=10 ms^{-1}), and cut-off wind speed is (V_{co}=52.5 ms^{-1}). The detailed set of PV and wind turbine parameters are obtained from the manufacturers' website (Kyocera, 2015; Aeolos, 2018), the battery parameter values are taken from Northrop et al. (2011) and the parameters for the degradation

Fig. 2. Schematic representation of a PV–wind battery hybrid power system.

model are taken from Ramadass et al. (2004). The main parameters of PV and wind turbine used for the system framework are mentioned in Table 2. AC load is assumed in this work, and the wind turbines are connected through an AC–DC converter as they generate AC power. The DC power generated from the PV panels is provided through the DC–AC inverter. A bidirectional DC–DC converter (combination of the boost–buck converter) facilitating charging and discharging integrates the BESS in the power system framework. The efficiency of the inverter (η_{inv}) is taken as 97%, and the voltage (V_{dc}) of 100 V is fixed across the DC bus. This paper studies the PV–wind battery hybrid power framework at the system level; therefore, a detailed internal design of power electronics components is not included. However, such details may easily be included in the present framework if required. Maximum power point tracking (MPPT) technique is used in the power control algorithm to extract the maximum possible power from PV panels and wind turbines at available solar irradiance and wind speed. The developed framework's power controller consists of DAE-based MPPT for PV panels (Lee et al., 2017; Bonkile and Ramadesigan, 2019) and rotor speed controlled MPPT for variable-speed wind turbines (Bonkile and Ramadesigan, 2022).

The lithium-ion battery's capacity loss may occur due to various reasons; one of them is undesirable side reactions resulting in the loss of cyclable lithium. The capacity fade model used in this work considers SEI layer formation and growth at the negative electrode–electrolyte interface (Ramadass et al., 2004). The equations for the side reaction current and the overpotential for the negative electrode are provided

Table 1

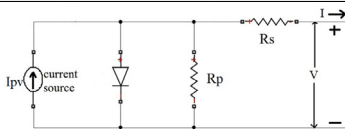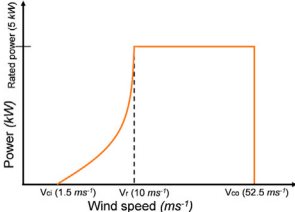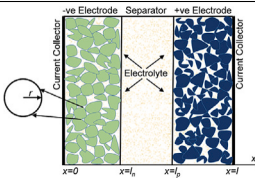Overview of system equations of the developed framework.

Equations	Schematic representation

PV cell model

PV output power: $P_{PV} = \eta_{inv} I V_{dc}$

I–V characteristics at MPP:

$$I = I_{PV} - I_o \left[\exp\left(\frac{V + R_s I}{V_{th} a} \right) - 1 \right] - \frac{V + R_s I}{R_p}; \quad \frac{I}{V} = \frac{I_o \left(1 - R_s \frac{I}{V} \right) \exp\left(\frac{V + R_s I}{V_{th} a} \right)}{V_{th} a} + \frac{1 - R_s \frac{I}{V}}{R_p}$$

Wind energy generation model

Wind turbine output power:

$$P_{WT} = \frac{1}{2} \rho A_{WT} V_w^3 C_p \eta_{inv} \eta_{mech}$$

$$P_{WT} = \begin{cases} 0, & V_w < V_{ci} \\ P_{WT}, & V_{ci} \le V_w \le V_r \\ P_{WT|Rated}, & V_r \le V_w \le V_{co} \\ 0, & V_w > V_{co} \end{cases}$$

Shaft speed at MPP:

$$\omega_{MPP} = \frac{V_w}{R_{WT}} \left(\frac{\alpha_1 \alpha_2 \alpha_6 (1 + \alpha_7 \alpha_8 \Theta + \Theta^3) + \alpha_7 \Theta (1 + \Theta^3)(\alpha_1 \alpha_2 + \alpha_1 \alpha_6 (\alpha_3 \Theta - \alpha_4 \Theta^\beta - \alpha_5))}{(1 + \Theta^3)(\alpha_1 \alpha_2 + \alpha_1 \alpha_6 (\alpha_3 \Theta - \alpha_4 \Theta^\beta - \alpha_5)) + \alpha_1 \alpha_2 \alpha_6 \alpha_8} \right)$$

Wind turbine power at MPP:

$$P_{WT|MPP} = 2.10 \times 10^{-3} \rho R_{WT}^5 \omega_{MPP}^3 \eta_{inv} \eta_{mech}$$

Physics-based battery model

Equations in −ve electrode (n), separator (s) and +ve electrode
(p): i = n, s, p

$$\nabla(\kappa_{eff,i} \nabla \phi_{e,i}) + \nabla[\kappa_{eff,i} \nabla ln(c_{e,i})] = -a_i j_i$$

$$\frac{\partial(\epsilon c_{e,i})}{\partial t} = \nabla(D_{eff,i}) + a_i (1 - t_+) j_i$$

Equations in −ve electrode (n) and +ve electrode (p): i = n, p

$$\nabla(\sigma_{eff,i} \nabla \phi_{s,i}) = a_i j_i; \quad \frac{\partial(\epsilon c_{s,i})}{\partial t} = \frac{D_{s,i}}{r^2} \frac{\partial}{\partial r} \left(r^2 \frac{\partial c_{s,i}}{\partial r} \right); \quad \eta_i = \phi_{s,i} - \phi_{e,i} - U_i - \frac{j_i}{a_i} R_{film}$$

$$j_i = k_{eff,i} c_{e,i}^{\alpha_a} \left(c_{s,i}^{max} - c_{s,i} \right)^{\alpha_a} c_{s,i}^{\alpha_c} \left[\exp\left(\frac{\alpha_a F}{RT} \eta_i \right) - \exp\left(-\frac{\alpha_c F}{RT} \eta_i \right) \right]$$

SEI layer formation and growth:

$$R_{film} = R_{SEI} + R_p(t); \quad R_p(t) = \frac{\delta_{film}}{\kappa_p}; \quad \frac{\partial \delta_{film}}{\partial t} = -\frac{j_s M_p}{a_n \rho_p F}; \quad R_{film}^{t+1} = R_{film}^t + R_p(t)^{t+1}$$

Table 2

Parameters used for the system framework.

Parameter	Symbol	Value
Wind energy generation system (Aeolos, 2018; Notton et al., 2001)		
Power law index	z	0.2
Mechanical components efficiency	η_{mech}	94%
Inverter efficiency	η_{inv}	97%
Number of blades		3
PV system (Lee et al., 2017; Kyocera, 2015)		
Series resistance	R_s	0.221 Ω
Parallel resistance	R_p	415.405 Ω
Series-connected cells	N_s	54
Current coefficient	K_I	0.0032 A K^{-1}
Nominal short-circuit voltage	$V_{oc,n}$	32.9 V
Nominal short-circuit current	$I_{sc,n}$	8.21 A
Voltage coefficient	K_v	−0.123 V K^{-1}
Light-generated current at the nominal condition	$I_{PV,n}$	8.214 A

in Table 1. It is assumed that this mode of degradation occurs only during the charging process. The increase in the SEI layer thickness increases the film resistance (R_{film}) leading to an increased potential drop across it, causing a fraction of the current being consumed in the side reaction and thus causing the capacity fade in the battery. This decreases recoverable capacity after each cycle, which is evident from the capacity curves (Fig. 7(c)). The cumulative capacity lost due to the side reaction is calculated, which provides the total capacity loss after an entire year of operation using the following equation.

$$Q_{lost} = \frac{Q_s}{Q_{max}} \times 100 \tag{1}$$

where Q_{max} is the initial rated capacity of the cell.

2.2. System sizing

The required number of PV panels (N_{PV}) and wind turbines (N_{WT}) are calculated as follows (Javed et al., 2020):

$$N_{PV} = \frac{Load_{DailyAvg}}{\eta_{bat} \times PV_{rated} \times s \times Losses} \tag{2}$$

$$N_{WT} = \frac{Load_{DailyAvg}}{\eta_{bat} \times Wind_{potential} \times A_{WT} \times Losses} \tag{3}$$

where $Load_{DailyAvg}$ is average daily load (kWh day^{-1}); PV_{rated} is rated output peak power of PV panel; panel generation factor s is 4.32; battery cyclic efficiency (η_{bat}) and overall loss factor ($Losses$) are assumed to be 90% and 15%, respectively; and $Wind_{potential}$ is wind energy potential (kWh m^{-2}day^{-1}) at the selected location. The difference between renewable energy generation and load demand decides the BESS size and associated energy storage cost. The total renewable power generated (P_{Total}) is a combination of PV panels (P_{PV}) and wind turbines (P_{WT}) power. The nominal BESS voltage is considered to be 48 V with 60% depth of discharge (DoD). The rate of energy change (dQ_c/dt) in the BESS is calculated using the power balance between the total energy generated (P_{Total}) and the load demand (P_{Load}) as follows (Roy et al., 2010):

$$\frac{dQ_c}{dt} = [P_{Total} - P_{Load}]\eta_{bat} \tag{4}$$

The change in stored energy for a relatively small time step Δt may be approximately written as:

$$Q_c(t + \Delta t) = Q_c(t) + [P_{Total} - P_{Load}]\eta_{bat}\Delta t \tag{5}$$

The required BESS capacity ($BESS_{cap}$) can be calculated as:

$$BESS_{cap} = \frac{\max[Q_c]}{DoD} \tag{6}$$

2.3. Power management and control strategy

In this section, a detailed description of efficient and cost-effective power management and control strategy is introduced for a PV–wind battery hybrid power system, as shown in Fig. 3. The power electronics components like inverters and bidirectional converters provide operational flexibility to satisfy the varying load demand. When the generated power is more than the demand, the excess power is used for battery charging using the bidirectional converter (buck mode). The power will be extracted from the battery through the same bidirectional converter (boost mode) during lower renewable power generation than the load demand. This synchronisation ensures uninterrupted power flow through the system to fulfil the load demand and charge/discharge the battery. Once the battery is fully charged, the control strategy shifts the operating point away from maximum power point while ensuring that the renewable power balances the demand and avoids the requirement of dump load systems thus achieving multiple objectives of the hybrid power systems. The developed control strategy has two operating modes, i.e. (a) MPPT mode and (b) controlled power generation (CPG) mode.

(a) *MPPT mode*: This is the default operating mode of the PV–wind battery hybrid power system. In this mode, the PV panels and wind turbines generate maximum power. If this generated power is equal to the load demand, then the BESS remains in the standby position. If the maximum generated renewable power ($P_{PV} + P_{WT}$) is inadequate to satisfy load demand, the BESS provides the rest of the power through the bidirectional converter. In this situation, the battery gets discharged, and its SoC decreases. On the other hand, if the maximum generated renewable power is more than the load demand, the available power is used to charge the battery if the battery SoC is less than 100%. The battery can store this power till SoC becomes 100%.

(b) *CPG mode*: The power control strategy shifts to this mode when the battery SoC is 100%, and the load demand is less than the total renewable power generation. Generally, the generation systems are operated at MPPT, and a dumping load system is installed to absorb this extra generated power, which adds to the system cost. The standalone PV–wind battery hybrid power system might not be required to generate maximum power throughout the year. Another objective of the proposed control strategy is to avoid a dumping load system requirement in dynamic operating conditions. The proposed power management and control strategy shifts the PV panel and wind turbine operation away from the MPP and generates only the required amount of power to satisfy the demand. The CPG mode prevents excess power generation to avoid power dumping and battery degradation due to overcharging. If the demand increases beyond the generated power, the control strategy shifts to the MPPT mode. All these aspects of the power control strategy are explained in detail in the results and discussion section.

2.4. Economic indices

The energy generation cost is considered as the main index to check the financial viability of the standalone PV–wind battery hybrid power system with different BESS size. The battery's actual life is taken based on the yearly degradation rate calculated using the P2D thermal battery model. Annualised Life Cycle Cost ($ALCC$) is calculated based on this life instead of the manufacturer provided fixed life and is mathematically represented as:

$$ALCC = C_0 \, CRF(d,n) + AC_{O\&M(battery)} + AC_{O\&M(PV+WT+BoS)} \tag{7}$$

$$CRF(d,n) = \frac{d(1+d)^n}{(1+d)^n - 1} \tag{8}$$

where C_0 is the total investment cost, $AC_{O\&M}$ is the annualised cost of operation and maintenance, $CRF(d,n)$ is the capital recovery factor, d is the discount rate, and n is the life of different components in the renewable hybrid power system. For life cycle costing, the life of PV panels, wind turbines and balance of system (BoS) are considered to be 25, 25 and 10 years, respectively. The discount rate is assumed as 10% and operation and maintenance cost is 1% of the capital cost. The BESS cost is taken as 24,090 ₹ kWh^{-1} (330 $ kWh^{-1}), BoS cost as 34,250 ₹ kWh^{-1} (469 $ kWh^{-1}), PV panels investment cost as 44,900 ₹ kWh^{-1} (615 $ kWh^{-1}) and wind turbine capital cost as 79,570 ₹ kWh^{-1} (1090 $ kWh^{-1}) (Cole and Frazier, 2019; Jacob et al., 2020; Kan et al., 2020). The energy generation cost (₹ kWh^{-1}) is calculated by dividing ALCC (₹) by annual energy demand (kWh).

3. Results and discussion

This section explains power control strategy and different scenarios (PV–wind mix), followed by the analysis of BESS size, degradation, and techno-economic study. The developed framework of a PV–wind battery hybrid power system is simulated in MATLAB® environment, and its performance is evaluated and discussed.

The hourly temperature, solar irradiation and wind speed data for a year (8760 data points) are considered for the performance analysis of the hybrid power system, as this data includes all the seasonal variations. The hourly solar irradiation, ambient temperature and wind speed data are provided by the European commission's photovoltaic geographical information system (PVGIS, 2020) for different locations in the world. Fig. 4 shows the average daily wind speed (dash–dot black line), temperature (blue line) and solar irradiation (dash red line) for twelve months at Hoshangabad (22.75 °N, 77.72 °E), India. The total renewable energy generation depends on the number of PV panels and wind turbines, whereas residential energy consumption defines the load demand curve. The power generated from the PV panels and wind turbines depends on solar irradiance and wind speed at the location.
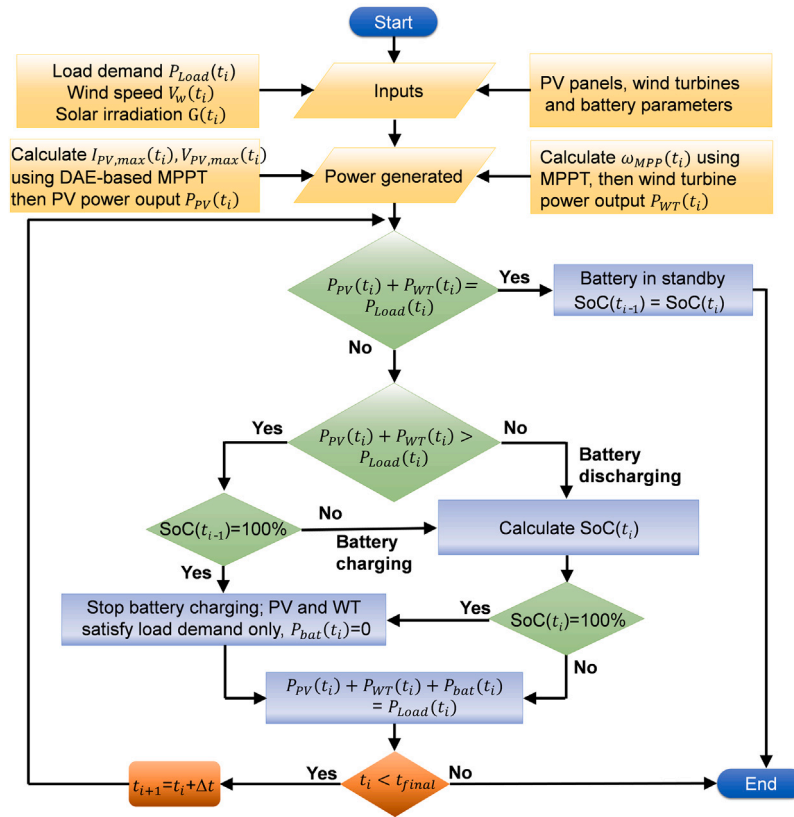
Fig. 3. Flow chart of proposed power management and control strategy.

The BESS is necessary due to the varying nature of solar irradiance and wind speed, affecting total renewable energy generation. The wind energy potential at Hoshangabad is 358 Wh m^{-2}day^{-1}. The selected location has comparatively low wind speed except for June–July; therefore, 5 kW rated power wind turbine (P_{Rated}) is chosen to be used in this study. The yearly energy consumption is considered to calculate the number of PV panels, wind turbines, and BESS size. The load demand curves are shown in Fig. 5 having an annual energy requirement of 142 MWh (Hourly Load Information, 2011). The average daily power generated by PV panels and wind turbines for twelve months under varying working conditions is shown in Fig. 5. The system component size is calculated for this locations' input data. However, the developed methodology is generic and can be applied to any location.

3.1. Power control strategy

Fig. 6 describes the power control strategy modes explained in Section 2.3. The working of MPPT and CPG mode is explained using 134th–136th and 172nd–174th day's results from the yearly simulation data. The positive BESS power values show the power supplied by the BESS during discharging operation. The negative BESS power indicates the power stored during the charging process. The BESS is mainly supplying power from 134th to 136th days, and therefore drop in SoC value (dotted green line) can be observed, as shown in Fig. 6(a). The power control strategy allows the renewable power sources to generate maximum power (MPPT mode) as the battery SoC value is less than 100%. The maximum generated renewable power is more than the load during 172nd to 174th days. This excess power ($P_{Total} - P_{Load}$) is stored in the BESS due to which the SoC value increases, as shown in Fig. 6(b). This process will continue till the battery SoC reaches its upper limit of a fully charged state (SoC = 100%). The encircled part of Fig. 6(b) indicates this state when no more power can be stored, and at this point, the renewable sources generate only the required amount

of power to satisfy demand (CPG mode). The power control strategy will shift to MPPT mode whenever the demand surges above generation capacity, and the BESS starts supplying power.

The excess power generated may destabilise the power flow of the system. These two operating modes of the power control strategy successfully achieve the desired power balance and ensure an uninterrupted power supply in all working conditions. A closer look reveals that the battery SoC value is not more than 100% in any case. This shows the satisfactory performance and robustness of the developed power management and control strategy.

3.2. Hybrid power system scenarios

Five scenarios of the PV–wind battery hybrid power system are considered to study the system performance and techno–economic analysis, as shown in Table 3. The same load demand profile and ambient conditions have been considered as input in all scenarios for comparative analysis. The total energy generated by the renewable hybrid system in a year is 142 MWh, and it is the same in all five scenarios. The first scenario includes 100% wind turbines, and no PV panels are considered. Power generated from PV panels is then included step by step, simultaneously reducing the wind turbine power percentage in the subsequent scenarios. Finally, in the last scenario, 100% PV power is considered with zero contribution from wind turbines.

For all five scenarios, the number of PV panels, wind turbines and BESS size is calculated using Eqs. (2), (3) and (6). As per the calculations, wind turbines of 450 kW$_p$ capacity are required for scenario I to satisfy the load demand. The required BESS capacity (1560 kWh) is the highest for scenario I with 100% wind turbines. This is due to the non-uniform wind speed throughout the year at the selected location. The wind turbine power generation is at the peak from June to August and at the lowest level during October to December (Fig. 5). This significant variation in wind turbine power generation results in
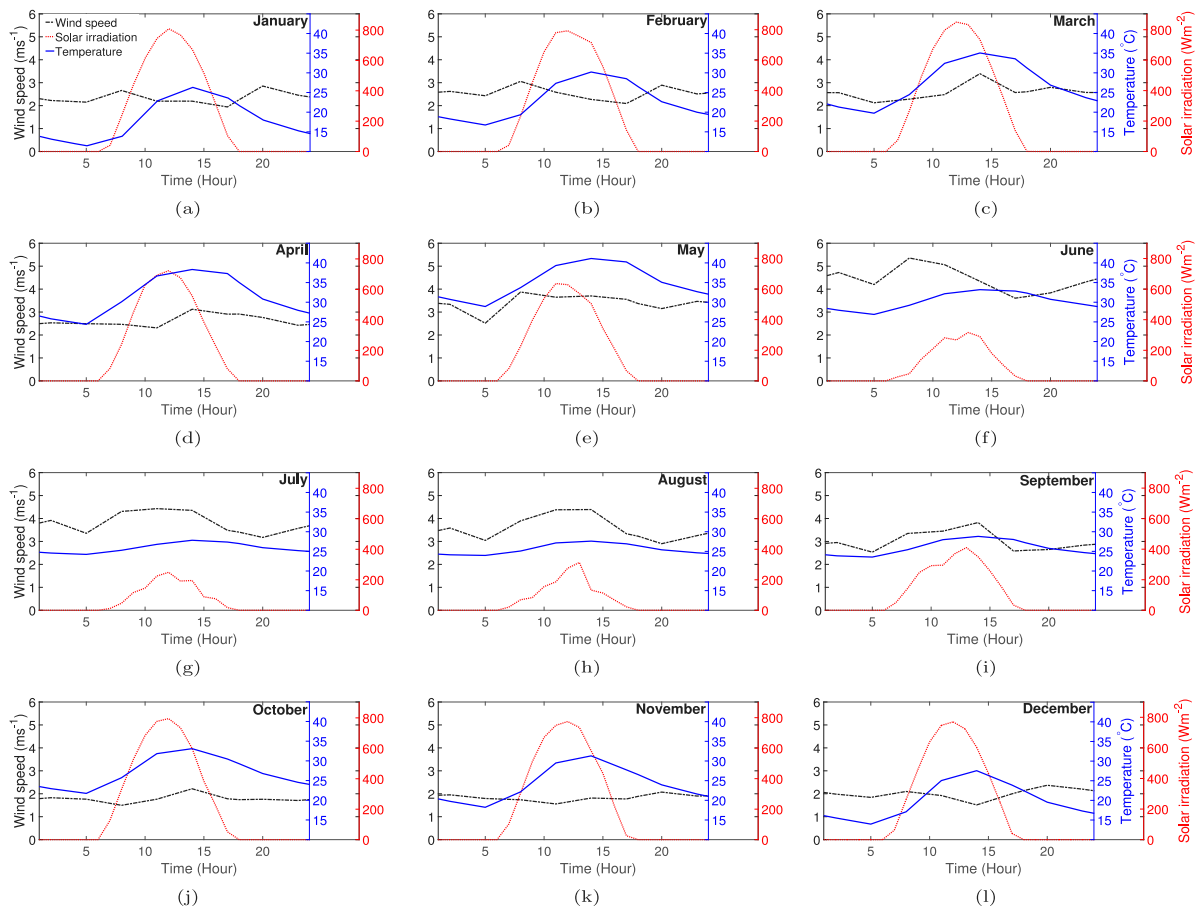
Fig. 4. Average daily wind speed (dash–dot black line), temperature (blue line) and solar irradiation (dash red line) at Hoshangabad (22.75 °N, 77.72 °E), India for each of the months.

Table 3
Scenario for PV–wind battery hybrid power system.

Scenario	Energy from WT	Energy from PV	Energy		
			WT (MWh)	PV (MWh)	BESS (kWh)
I	100%	0%	142	0	1560
II	70%	30%	99.4	42.6	990
III	50%	50%	71	71	605
IV	30%	70%	42.6	99.4	350
V	0%	100%	0	142	940

a mismatch between load demand and power generation. Hence, a large BESS is needed to balance the energy difference in the scenario I compared to other scenarios. The minimum and maximum PV panels capacities are 36 kW$_p$ (Scenario II) and 119 kW$_p$ (Scenario V). The battery energy storage requirement reduces as PV energy generation is included into the renewable hybrid power system. The PV energy generation is comparatively more balanced, i.e., availability of solar ir-radiance during daytime guarantees the energy generation. Scenario IV with 30% wind turbine and 70% PV panel energy generation requires the least BESS capacity (350 kWh) compared to other scenarios.

3.3. Techno–economic analysis

Simulations of the developed framework and techno–economic analysis to study the impact of BESS size variation on the degradation and cost of energy generation is done for all the five scenarios, as listed in Table 3. Fig. 7 shows SoC range, energy generation cost, degradation rate, and capacity lost for a year, which provides detailed insights into the size-degradation-cost interdependence. The BESS size is calculated as explained in Section 2.2 and mentioned in Table 3

for all the scenarios. This value is considered as the base case storage capacity for size variations. The developed framework is simulated for different BESS sizes (95%, 100% (base case), 110%, 120%, 130%, 140%, and 150%), keeping other parameters constant. For the current conditions, the BESS gets discharged entirely (0% SoC) if the BESS size is reduced by more than 5% from the base case. Hence, 95% BESS size is considered as the lower bound.

In this work, we divide the battery SoC values into three ranges; SoC greater than 70% as 'High', 40% to 70% as 'Mid' and less than 40% as 'Low', as shown in Fig. 7(a) for all scenarios.

Fig. 7(b) shows the degradation rate (% year^{-1}) on primary y-axis and energy generation cost (₹ kWh^{-1}) on secondary y-axis for all scenarios. In all the scenarios, the battery degradation rate (black dotted line) decreases with an increment in the BESS size. Fig. 7(c) shows the degradation rate throughout the year for three representative BESS sizes for all scenarios. The rate of degradation is more at higher cell potentials (i.e. high SoC). Hence, operating the BESS at lower SoC prevents degradation to a certain extent. The oversized BESS can be operated at lower SoC for more operational hours, avoiding rapid degradation at high potentials. This results in lesser capacity fade and
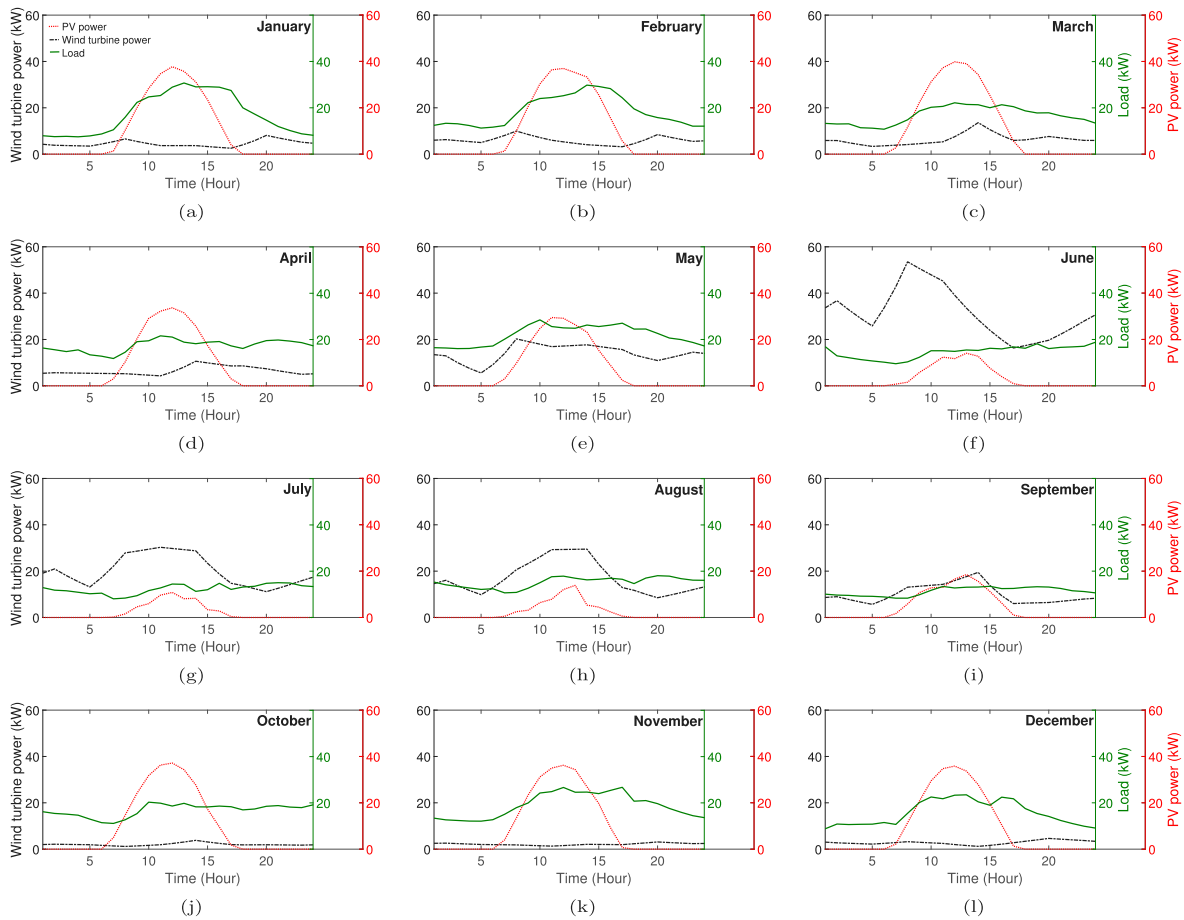
Fig. 5. Average daily load profile (green line), PV (dash red line) and wind turbine power (dash–dot black line) at Hoshangabad (22.75 °N, 77.72 °E), India for each of the months.
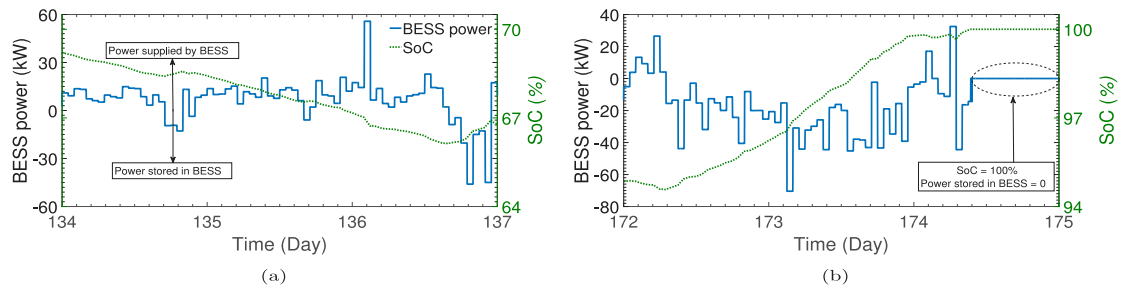

Fig. 6. Power management and control strategy: (a) MPPT mode; (b) CPG mode.

extended life in oversized BESS as compared to the base case. The energy generation cost is the maximum for the scenario with 100% WT, i.e. ₹121 (1.657 $) to ₹130 (1.780 $) per kWh as shown in Fig. 7(b). This is due to the low wind potential at the selected location, and thus a large number of wind turbines being installed. Increasing the BESS size by 20% from the base size improves life from 4.4 years (base size) to 5.8 years, thus reducing the energy generation cost from ₹124.22 (1.701 $)) to ₹121.33 (1.662 $) per kWh. The energy generation cost decreases with the increase in PV share in the hybrid power system for the chosen location. In scenario III, a 30% increase in BESS size from the base case improves the battery life by ≈2 years and thus reduces the energy generation cost from ₹63.4 (0.868 $) (base size) to ₹60.05 (0.822 $) per kWh. The simulation results of all the scenarios show similar trends qualitatively. Scenario IV (30% WT and 70% PV) is a better configuration from an economic aspect because of the least energy generation cost for the selected location. Higher PV

power contribution (70%) complemented by wind turbine power (30%) results in lower BESS capacity in this scenario. This also highlights the fact that system hybridisation reduces the energy generation cost significantly. Henceforth the results of scenario IV are used for further discussions.

As per the system sizing calculations, scenario IV needs 135 kW$_p$ wind turbines, 83 kW$_p$ PV panels and 350 kWh BESS (base case). The battery SoC value increases up to 100% during charging and operates for 2295 h in the High SoC range for the base size case, as shown in Table 4. For the subsequent two cases, the SoC value is in the High SoC range for 1724 and 373 h for 110% and 120% BESS size, respectively. The increase in BESS size reduces the number of hours in the High SoC range, thereby reducing the battery degradation rate. After a 30% increase in the BESS size, the SoC values are only in the Mid and Low SoC ranges. The capacity loss is maximum for 95% BESS size (3.90% year^{-1}) and continuously declines with an increase in BESS size.
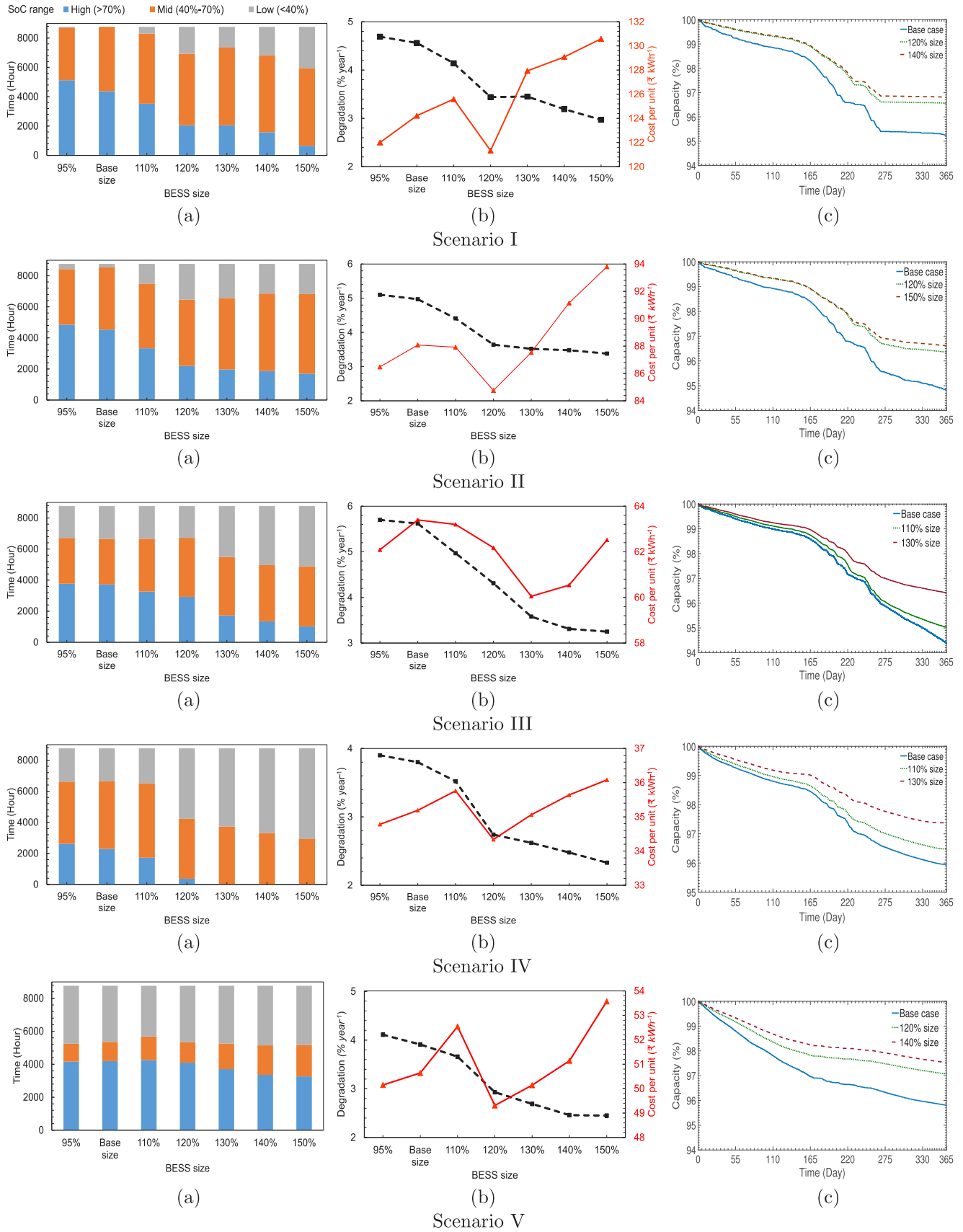
Fig. 7. (a) SoC range; (b) Energy generation cost and degradation rate; (c) Capacity lost.

Table 4
Size-degradation-cost interdependence for scenario IV (30% WT and 70% PV)

BESS size	High SoC (h)	Degradation (% year^{-1})	Generation cost (₹ kWh^{-1})
95%	2614	3.90	34.78
100%	2295	3.80	35.19
110%	1724	3.52	35.76
120%	373	2.74	34.34
130%	0	2.62	35.06
140%	0	2.48	35.64
150%	0	2.33	36.08

The degradation rate is 3.80%, 3.52%, 2.74%, 2.62%, 2.48%, 2.33% per year for every 10% increment in the BESS size, as shown in Table 4. As the degradation rate decreases, the battery life increases. Therefore, an increase in BESS size provides more service life compared to the base case.

The energy generation cost for the base case is 35.19 ₹ kWh^{-1} (0.482 $ kWh^{-1}) with ₹5,104,966 (69,931 $) *ALCC* and the degradation rate is 3.8% per year, as shown in Table 4. In this case, the battery life would be approximately 5.3 years. The energy generation cost for 120% BESS size is 34.34 ₹ kWh^{-1} (0.470 $ kWh^{-1}) (₹4,875,680 (66,790 $) *ALCC*) with corresponding degradation rate of 2.74% per year (i.e., ≈7.3 year life). This noticeable reduction in the energy generation cost for 120% BESS size is attributed to the lower degradation rate and, therefore, longer battery life under the same ambient and operating conditions. Though the degradation rate decreases on increasing the BESS size beyond 120%, the energy generation cost starts rising. This is because, after this point, the investment cost becomes more dominant than the CRF (Eq. (7)), and, therefore, the improvement in battery life does not help to reduce the cost. As shown in Fig. 7 scenario IV (c), the BESS has degraded with varying rates in a year. Rapid battery degradation is observed from 180 to 240 days. This can be attributed to a large amount of renewable energy being stored resulted in higher battery SoC. As per the simulation results, the 20% increase in BESS size reduces the degradation from 3.80% to 2.74% per year (≈38% more life) and the energy generation cost from ₹35.19 (0.482 $) to ₹34.34 (0.470 $) per kWh. This study indicates the potential benefits of BESS size increment in PV–wind battery hybrid power systems, in turn reducing the degradation and energy generation cost.

Here, the results obtained by simulating the proposed renewable hybrid power system framework are compared qualitatively with previous studies available in the literature. Ghorbani et al. (2018) optimised a standalone PV–wind battery hybrid power system to minimise the net present cost and calculated the levelized cost of energy to be 0.508 $ kWh^{-1} without considering dynamic battery degradation in their yearly simulations. Kumar and Saini (2020) used the salp swarm algorithm to optimise a standalone hybrid renewable energy system to compare three BESS technologies and minimise energy generation costs. The simulation results showed that the lithium-ion BESS has an energy generation cost of 0.636 $ kWh^{-1}; however, they did not account for battery degradation. In comparison, based on the calculations performed using the proposed framework, including battery degradation, the energy generation cost is 0.470 $ kWh^{-1} while using 120% of the required BESS size. The BESS size depends on renewable power generation and load demand, which are directly related to the specific location. Therefore, every location will have a different BESS size. Though the proposed approach is illustrated for an Indian city, it may be extended to any location irrespective of load, power generation and BESS size. However, the findings of this study have to be seen in light of some limitations. The uncertainties in ambient conditions and user demand are not considered in the simulations. The degradation mechanisms in solar cell and wind energy generation system is not included in the developed framework. The component failures of power electronic systems may happen during the long term operation, which is not incorporated in the analysis. These insights will help better life predictions, policymaking for BESS deployment and improve the financial feasibility of deploying PV–wind battery hybrid power systems.

4. Conclusions

The PV–wind battery hybrid power system framework is developed and simulated under varying operating conditions. The physics-based P2D thermal battery model is used to study degradation due to SEI layer formation and growth. Fig. 7(b) indicates that the degradation mechanism (cell level) has a significant impact on the energy generation cost (system level). The simulation results presented in this paper push the boundaries of BESS modelling strategies from being just a black-box approach. The power management and control strategy with maximum power point tracking (MPPT) mode and controlled power generation (CPG) mode is developed and found to be reliable and efficient under real-world operating conditions. The developed framework is evaluated for five different scenarios of the PV and wind turbine (WT) power generation mix. This paper is an important step towards understanding the BESS behaviour and degradation using a physics-based P2D thermal battery model and its impact on the energy generation cost of PV–wind battery hybrid power systems. The illustrative results of this work led to three key findings:

- The results show that the proposed power control strategy with MPPT and CPG mode satisfies the objectives of PV–wind battery hybrid power systems such as maximum power generation, avoid battery overcharging, and zero dumped power. The physics-based P2D thermal model for lithium-ion battery performance simulation is demonstrated as a proof of concept for accurate prediction, robust control of the BESS.

- This work demonstrates a simple and effective method of improving the financial feasibility of renewable hybrid power systems. The BESS with increased size from the base case can be operated in the High SoC range for fewer hours, resulting in lesser degradation and longer life. From the simulation results presented, it can be inferred that the increased BESS size can reduce the energy generation cost of the PV–wind battery hybrid power system if battery degradation is considered.

- This work examines battery life extension using a simple BESS sizing strategy considering a physics-based battery model with degradation. We found the battery life improvement of ≈38% with an increased BESS size. The results show that the 20% increase in the BESS size can significantly reduce the degradation from 3.80% year^{-1} to 2.74% year^{-1} and the energy generation cost from 35.19 ₹ kWh^{-1} (0.482 $ kWh^{-1}) to 34.34 ₹ kWh^{-1} (0.470 $ kWh^{-1}) for scenario IV.

The yearly simulation results and the physics-based battery models facilitate better degradation modelling to predict battery life are beneficial to understand the effects of BESS sizing on its life and energy generation cost of PV–wind battery hybrid power systems. The developed framework could be extended for better battery design and performance optimisation and to improve safety and reliability in the future. A more detailed investigation is required to incorporate uncertainties in ambient conditions and load demand. Efficient simulation of renewable energy sources and storage technologies can be implemented in the proposed framework to design better renewable hybrid power systems. These findings provide techno–economic insights to policymakers and commercial renewable power producers. This work does not consider the environmental impact of renewable hybrid power systems with BESS in general and specifically the effect of the increased size. Such impact analysis would be an attractive study and may be attempted in the future. Renewable hybrid power systems are essential for a sustainable society, and BESS can significantly improve the reliability of renewable power systems and their penetration in the electricity generation sector.

List of symbols

$ALCC$	annualised life cycle cost, [₹(US $)]
A_{WT}	rotor swept area, m^2
a	diode ideality constant
a_i	particle surface area to volume, [m^2 m^{-3}]
$BESS_{cap}$	required battery energy storage capacity, [kWh]
c_e	electrolyte concentration, [mol m^{-3}]
c_s	solid-phase concentration, [mol m^{-3}]
D_{eff}	Effective electrolyte diffusion coefficient, [m^2 s^{-1}]
D_s	Effective solid-phase diffusion coefficient, [m^2 s^{-1}]
F	Faraday's constant, 96,487 C mol^{-1}
M_p	molecular weight of products formed as a result of side reaction, [molkg^{-1}]
i_{o_s}	side reaction exchange current density, [Am^{-2}]
I	output current, [A]
I_{PV}	PV current, [A]
I_o	saturation current, [A]
j	ionic flux, [mol m^{-2} s^{-1}]
k_{eff}	effective reaction rate, m$^{2.5}$ mol$^{-0.5}$ s^{-1}
P_{Load}	load demand, [kW]
P_{PV}	PV panel output power, [kW]
P_{Total}	total renewable power, [kW]
$P_{WT|Rated}$	wind turbine rated power, kW
$P_{WT|MPP}$	wind turbine power at MPP, [kW]
P_{WT}	wind turbine output power, [kW]
Q_c	BESS energy, [kWh]
R_{WT}	rotor radius, [m]
R	ideal gas constant, 8.3143 Jmol^{-1} K^{-1}
R_{film}	film resistance at the electrode/electrolyte interface, [Ω m^2]
R_{SEI}	resistance of the SEI formed initially during the formation period, [Ω m^2]
R_s	series resistance, [Ω]
R_p	parallel resistance, [Ω]
T	temperature of the cell, [K]
$U_{s,ref}$	open circuit potential for the solvent reduction reaction [V]
V	output voltage, [V]
V_{ci}	cut-in wind speed, m s^{-1}
V_{co}	cut-out wind speed, m s^{-1}
V_{dc}	DC bus voltage, [V]
V_r	rated wind speed, [m s^{-1}]
V_{th}	thermal voltage, [V]
V_w	wind speed at a hub height, [m s^{-1}]

Greek

ρ	air density, 1.22 kg m^{-3}
ρ_p	density of products formed as a result of side reaction, [kg m^{-3}]
$\phi_{s,e}$	local potential of a phase, (s = solid; e = liquid), [V]
σ_{eff}	effective solid-phase conductivity, [S m^{-1}]
κ_{eff}	effective electrolyte conductivity, [S m^{-1}]
ϵ	porosity
η_{inv}	inverter efficiency, 94%
η_{mech}	mechanical efficiency, 97%
η	over potential, [V]
Θ	pitch angle
ω	turbine shaft speed
ω_{MPP}	turbine shaft speed at MPP
δ_{film}	film thickness, [m]
Δt	time step, [s]
κ_p	conductivity, [S m^{-1}]

CRediT authorship contribution statement

Mayur P. Bonkile: Software, Validation, Formal analysis, Investigation, Data curation, Writing – original draft, Visualization. **Venkatasailanathan Ramadesigan:** Conceptualization, Methodology, Resources, Writing – review & editing, Supervision, Project administration, Funding acquisition.

Declaration of competing interest

The authors declare that they have no known competing financial interests or personal relationships that could have appeared to influence the work reported in this paper.

Acknowledgements

References

Aeolos, 2018. Aeolos-v 5kw wind turbine datasheet. https://en.wind-turbine-models.com/turbines/1853-aeolos-aeolos-v-5kw. (Accessed 31 January 2020).

Al-Sharafi, A., Sahin, A.Z., Ayar, T., Yilbas, B.S., 2017. Techno-economic analysis and optimization of solar and wind energy systems for power generation and hydrogen production in Saudi Arabia. Renew. Sustain. Energy Rev. 69, 33–49.

Altun, A.F., Kilic, M., 2020. Design and performance evaluation based on economics and environmental impact of a PV-wind-diesel and battery standalone power system for various climates in Turkey. Renew. Energy 157, 424–443.

Arabi-Nowdeh, S., Nasri, S., Saftjani, P.B., Naderipour, A., Abdul-Malek, Z., Kamyab, H., Jafar-Nowdeh, A., 2021. Multi-criteria optimal design of hybrid clean energy system with battery storage considering off- and on-grid application. J. Clean. Prod. 290, 125808.

Bakay, M.S., Ümit Ağbulut, 2021. Electricity production based forecasting of greenhouse gas emissions in Turkey with deep learning, support vector machine and artificial neural network algorithms. J. Clean. Prod. 285, 125324.

Balducci, P.J., Alam, M.J.E., Hardy, T.D., Wu, D., 2018. Assigning value to energy storage systems at multiple points in an electrical grid. Energy Environ. Sci. 11, 1926–1944.

Birkl, C.R., Roberts, M.R., McTurk, E., Bruce, P.G., Howey, D.A., 2017. Degradation diagnostics for lithium ion cells. J. Power Sources 341, 373–386.

Bonkile, M.P., Ramadesigan, V., 2019. Power management control strategy using physics-based battery models in standalone PV-battery hybrid systems. J. Energy Storage 23, 258–268.

Bonkile, M.P., Ramadesigan, V., 2020. Physics-based models in PV-battery hybrid power systems: Thermal management and degradation analysis. J. Energy Storage 31, 101458.

Bonkile, M.P., Ramadesigan, V., 2022. Power control strategy and economic analysis using physics-based battery models in standalone wind-battery systems.

Cebulla, F., Haas, J., Eichman, J., Nowak, W., Mancarella, P., 2018. How much electrical energy storage do we need? A synthesis for the U.S., Europe, and Germany. J. Clean. Prod. 181, 449–459.

Cole, W., Frazier, A.W., 2019. Cost Projections for Utility-Scale Battery Storage. vol. NREL/TP-6A20-73222, National Renewable Energy Laboratory.

Deshmukh, M., Deshmukh, S., 2008. Modeling of hybrid renewable energy systems. Renew. Sustain. Energy Rev. 12 (1), 235–249.

Doyle, M., Newman, J., Gozdz, A.S., Schmutz, C.N., Tarascon, J.-M., 1996. Comparison of modeling predictions with experimental data from plastic lithium ion cells. J. Electrochem. Soc. 143 (6), 1890–1903.

Edge, J.S., O'Kane, S., Prosser, R., Kirkaldy, N.D., Patel, A.N., Hales, A., Ghosh, A., Ai, W., Chen, J., Yang, J., Li, S., Pang, M.-C., Bravo Diaz, L., Tomaszewska, A., Marzook, M.W., Radhakrishnan, K.N., Wang, H., Patel, Y., Wu, B., Offer, G.J., 2021. Lithium ion battery degradation: What you need to know. Phys. Chem. Chem. Phys. 23, 8200–8221.

Fayaz, H., Afzal, A., Samee, A.D.M., Soudagar, M.E.M., Akram, N., Mujtaba, M.A., Jilte, R.D., Islam, M.T., Ümit Ağbulut, Saleel, C.A., 2021. Optimization of thermal and structural design in lithium-ion batteries to obtain energy efficient battery thermal management system (BTMS): A critical review. Arch. Comput. Methods Eng. 2943.

Fragaki, A., Markvart, T., Laskos, G., 2019. All UK electricity supplied by wind and photovoltaics – The 30–30 rule. Energy 169, 228–237.

Ghorbani, N., Kasaeian, A., Toopshekan, A., Bahrami, L., Maghami, A., 2018. Optimizing a hybrid wind-PV-battery system using GA-PSO and MOPSO for reducing cost and increasing reliability. Energy 154, 581–591.

Hannan, M., Al-Shetwi, A., Begum, R., Young, S., Hoque, M., Ker, P., Mansur, M., Alzaareer, K., 2020. The value of thermal management control strategies for battery energy storage in grid decarbonization: Issues and recommendations. J. Clean. Prod. 276, 124223.

Harris, S.J., Harris, D.J., Li, C., 2017. Failure statistics for commercial lithium ion batteries: A study of 24 pouch cells. J. Power Sources 342, 589–597.

Hourly Load Information, 2011. Hourly feeder load information: maharashtra state electricity distribution co. ltd.. https://www.mahadiscom.in/en/hourly-feeder-load-information/. (Accessed 15 December 2020).

IEA, 2020. Global energy review 2019. International Energy Agency (IEA), Paris.

Jacob, A.S., Banerjee, R., Ghosh, P.C., 2020. Trade-off between end of life of battery and reliability in a photovoltaic system. J. Energy Storage 30, 101565.

Javed, M.S., Zhong, D., Ma, T., Song, A., Ahmed, S., 2020. Hybrid pumped hydro and battery storage for renewable energy based power supply system. Appl. Energy 257, 114026.

Kan, X., Hedenus, F., Reichenberg, L., 2020. The cost of a future low-carbon electricity system without nuclear power – The case of Sweden. Energy 195, 117015.

Koohi-Fayegh, S., Rosen, M., 2020. A review of energy storage types, applications and recent developments. J. Energy Storage 27, 101047.

Kumar, P.P., Saini, R.P., 2020. Optimization of an off-grid integrated hybrid renewable energy system with different battery technologies for rural electrification in India. J. Energy Storage 32, 101912.

Kyocera, 2015. Kyocera kc200gt high efficiency multicrystal photovoltaic module datasheet. https://www.energymatters.com.au/images/kyocera/KC200GT.pdf. (Accessed 10 January 2020).

Lee, S.B., Pathak, C., Ramadesigan, V., Gao, W., Subramanian, V.R., 2017. Direct, efficient, and real-time simulation of physics-based battery models for stand-alone PV-battery microgrids. J. Electrochem. Soc. 164 (11), E3026–E3034.

Li, J., Adewuyi, K., Lotfi, N., Landers, R., Park, J., 2018. A single particle model with chemical/mechanical degradation physics for lithium ion battery state of health (SOH) estimation. Appl. Energy 212, 1178–1190.

Li, C., Zhou, D., Wang, H., Lu, Y., Li, D., 2020. Techno-economic performance study of stand-alone wind/diesel/battery hybrid system with different battery technologies in the cold region of China. Energy 192, 116702.

Liu, Z., Ivanco, A., Onori, S., 2019. Aging characterization and modeling of nickel-manganese-cobalt lithium-ion batteries for 48V mild hybrid electric vehicle applications. J. Energy Storage 21, 519–527.

Mazzeo, D., Matera, N., De Luca, P., Baglivo, C., Congedo, P.M., Oliveti, G., 2021. A literature review and statistical analysis of photovoltaic-wind hybrid renewable system research by considering the most relevant 550 articles: An upgradable matrix literature database. J. Clean. Prod. 295, 126070.

Murugaperumal, K., Ajay D. Vimal Raj, P., 2019. Feasibility design and techno–economic analysis of hybrid renewable energy system for rural electrification. Sol. Energy 188, 1068–1083.

NITI Aayog, 2021. Energy storage system roadmap for India: 2019 – 2032. https://www.niti.gov.in/sites/default/files/2019-11/ISGF.pdf. (Accessed 13 May 2021).

Northrop, P.W.C., Ramadesigan, V., De, S., Subramanian, V.R., 2011. Coordinate transformation, orthogonal collocation, model reformulation and simulation of electrochemical-thermal behavior of lithium-ion battery stacks. J. Electrochem. Soc. 158 (12), A1461–A1477.

Notton, G., Muselli, M., Poggi, P., Louche, A., 2001. Decentralized wind energy systems providing small electrical loads in remote areas. Int. J. Energy Res. 25, 141–164.

Onori, S., Lee, S.B., 2019. Optimizing energy and cost in renewable grid systems: An electrochemistry and control-based idea. R&D world, https://www.rdworldonline.com/optimizing-energy-and-cost-in-renewable-grid-systems-an-electrochemistry-and-control-based-idea. (Accessed 10 October 2020).

Ortega-Arriaga, P., Babacan, O., Nelson, J., Gambhir, A., 2021. Grid versus off-grid electricity access options: A review on the economic and environmental impacts. Renew. Sustain. Energy Rev. 143, 110864.

Peled, E., 1979. The electrochemical behavior of alkali and alkaline earth metals in non-aqueous battery systems—The solid electrolyte interphase model. J. Electrochem. Soc. 126 (12), 2047–2051.

Peled, E., Golodnitsky, D., Ardel, G., 1997. Advanced model for solid electrolyte interphase electrodes in liquid and polymer electrolytes. J. Electrochem. Soc. 144 (8), L208–L210.

PVGIS, 2020. Photovoltaic geographical information system - pv performance tool. http://re.jrc.ec.europa.eu/pvg_tools#PVP. (Accessed 15 October 2020).

Rahimian, S.K., Rayman, S., White, R.E., 2011. Comparison of single particle and equivalent circuit analog models for a lithium-ion cell. J. Power Sources 196 (20), 8450–8462.

Rallo, H., Canals Casals, L., De La Torre, D., Reinhardt, R., Marchante, C., Amante, B., 2020. Lithium-ion battery 2nd life used as a stationary energy storage system: Ageing and economic analysis in two real cases. J. Clean. Prod. 272, 122584.

Ramadass, P., Haran, B., Gomadam, P.M., White, R., Popov, B.N., 2004. Development of first principles capacity fade model for li-ion cells. J. Electrochem. Soc. 151 (2), A196–A203.

Ramadesigan, V., Northrop, P.W.C., De, S., Santhanagopalan, S., Braatz, R.D., Subramanian, V.R., 2012. Modeling and simulation of lithium-ion batteries from a systems engineering perspective. J. Electrochem. Soc. 159 (3), R31–R45.

Roy, A., Arun, P., Bandyopadhyay, S., 2007. Design and optimization of renewable energy based isolated power systems. SESI J. 17 (1), 1–16.

Roy, A., Kedare, S.B., Bandyopadhyay, S., 2009. Application of design space methodology for optimum sizing of wind–battery systems. Appl. Energy 86 (12), 2690–2703.

Roy, A., Kedare, S.B., Bandyopadhyay, S., 2010. Optimum sizing of wind-battery systems incorporating resource uncertainty. Appl. Energy 87 (8), 2712–2727.

Safari, M., Morcrette, M., Teyssot, A., Delacourt, C., 2009. Multimodal physics-based aging model for life prediction of li-ion batteries. J. Electrochem. Soc. 156.

Schimpe, M., von Kuepach, M.E., Naumann, M., Hesse, H.C., Smith, K., Jossen, A., 2018. Comprehensive modeling of temperature-dependent degradation mechanisms in lithium iron phosphate batteries. J. Electrochem. Soc. 165 (2), A181–A193.

Schmalstieg, J., Käbitz, S., Ecker, M., Sauer, D.U., 2014. A holistic aging model for Li(NiMnCO)O2 based 18650 lithium-ion batteries. J. Power Sources 257, 325–334.

Sreeraj, E., Chatterjee, K., Bandyopadhyay, S., 2010. Design of isolated renewable hybrid power systems. Sol. Energy 84 (7), 1124–1136.

Torchio, M., Magni, L., Gopaluni, R.B., Braatz, R.D., Raimondo, D.M., 2016. LION-SIMBA: A MATLAB framework based on a finite volume model suitable for li-ion battery design, simulation, and control. J. Electrochem. Soc. 163 (7), A1192–A1205.